

# Nonlinear Schrödinger Kernel Computing for Ultrafast Single-shot Data Acquisition and Inference

Bahram Jalali, Tingyi Zhou, Fabien Scalzo

*Electrical and Computer Engineering Department, UCLA*

*jalali@ucla.edu*

**Abstract:** We introduce the concept of Nonlinear Schrödinger Kernel Computing – a method that accelerates inference by nonlinear transformation of spectrally modulated data. Experimental results and applications to time stretch microscopy and nonlinear classification are demonstrated. © 2021 The Author(s)

## 1. Introduction

Deep learning’s insatiable demand on computing power and massive data sets calls for fresh approaches to machine intelligence that are computationally light succeed with only a small training dataset and offer low latency. The paper shows how nonlinear spectral dynamics that underpin phenomena in nature such as optical rogue waves and supercontinuum generation [1] [2] [3] [4] can be leveraged to accelerate machine learning. We show that complex optical dynamics transform a difficult nonlinear classification problem into a simple linear separation task that can be done using a very simple low-latency linear classifier - instead of a complex nonlinear classifier [5]. The technique we call Nonlinear Schrödinger Kernel is an entirely new approach to computing and inference and is validated in a number of experiments. This work builds on more than two decades of research on time stretch instruments [6] [7] [8] [9] and its utility in studies of extreme nonlinear dynamics including the Optical Rogue Waves [1]; dynamics of soliton molecule [10], and analog optical computing [11]. Our approach starts by modulating the data onto the optical spectrum of a femtosecond pulse and then using it to seed nonlinear optical dynamics. Acting as a spectrally-modulated data packet, the femtosecond pulse is transformed through a nonlinear medium before being captured by a spectrometer and passed to a digital linear classifier [5]. This process projects linearly non-separable data to a space where they become linearly separable. We validate this intuition by performing a nonlinear classification benchmark task (XOR operation), followed by the classification of time stretch microscopy images. We show that from a functional perspective, our system performs kernel computing but with a kernel that is physical and has dramatically lower latency than the popular numerical kernel employed in machine learning. Since the data is first modulated onto the optical spectrum, this technique is fully compatible with time stretch data acquisition [9] for fast single-shot and continuous operation.

## 2. Experiment

The experimental system is shown in fig. 1. It consists of a fiber-based supercontinuum laser source, a spectral modulator, a nonlinear optical element, and the spectrum readout followed by a machine learning classifier operating in digital domain. The data is modulated onto the laser spectrum through the spectral modulator. The modulated waveform then passes through a nonlinear optical element where nonlinear transformation takes place. We define the combination of the spectral modulation of the data and its nonlinear transformation as the Nonlinear Schrödinger Kernel. Because of the spectral nature of this Kernel, this can also be called Lambda Kernel, in homage to the convention of representing wavelengths with the symbol lambda ( $\lambda$ ) [5]. The optical spectrum after Nonlinear Schrödinger Kernel is read out, digitized and fed into machine learning. The spectrum readout shown in fig. 1b can either be a traditional grating-based spectrometer or time stretch spectrometer [12] for fast single-shot operation. Both techniques are demonstrated in this work.

## 3. Results

The effectiveness of this approach is evaluated through various experimental protocols. An interesting property of the Nonlinear Schrödinger Kernel is to project the original signal into a modified space that emphasizes certain

nonlinear properties of the data. In terms of functionality, similarities exist between the Nonlinear Schrödinger Kernel and the concept of “kernel projection” or “kernel trick” in the machine learning literature. The utility of such a processing method is to transform data that is not linearly separable so it becomes linearly separable in the new space.

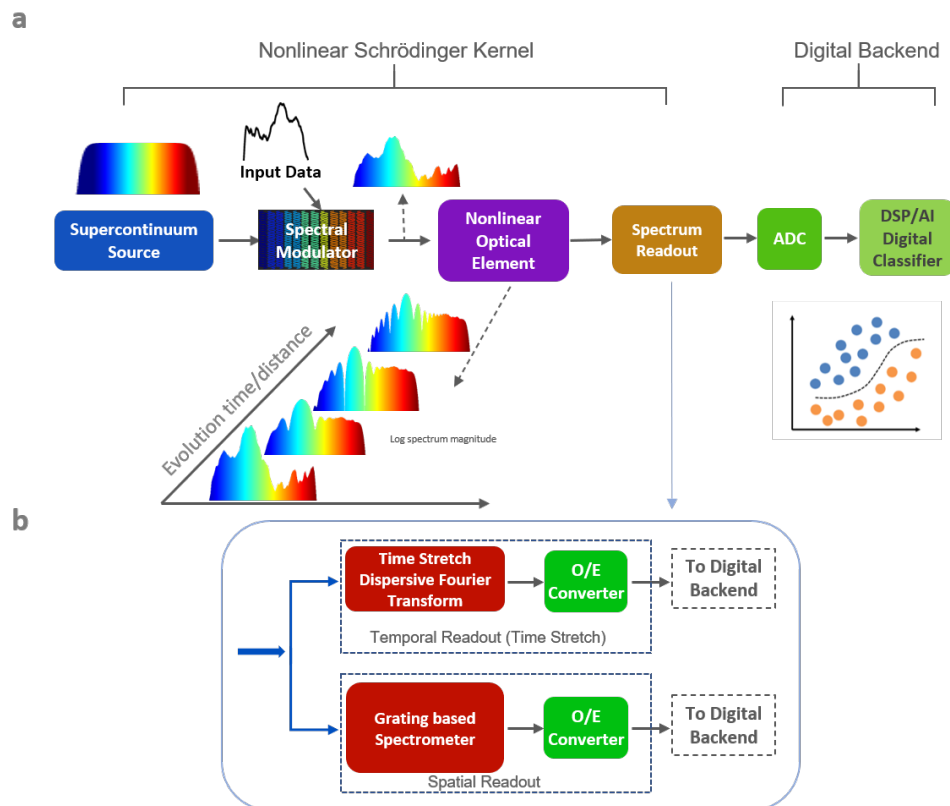


Fig. 1: (a) Simplified block diagram showing the basic building blocks of the Nonlinear Schrödinger Kernel Computing system. In the experiments, a broadband (supercontinuum) pulsed laser is used as the source. The data is modulated onto the optical spectrum and the modulated waveform is transformed by nonlinear propagation in an optical media. The inset shows the nonlinear evolution seeded by the data-modulated spectrum. The spectrum at the output is read out and sent to a digital classifier for classification. (b) The spectrum readout can either be performed by a conventional spectrometer based on diffraction gratings, or by using time stretch spectroscopy for fast single-shot performance. Classification is performed using a machine learning algorithm in the digital domain.

We first illustrate this property by performing the Exclusive OR (XOR) task which is a classic problem that cannot be performed with a linear model and often serves as a benchmark for nonlinear classification. Given four data points representing the binary input pairs  $([0,0], [0,1], [1,0], [1,1])$  and their corresponding XOR output  $(0,1,1,0)$  as training, a linear classifier will inevitably lead to error when attempting to reproduce the results of the XOR operation (as illustrated in fig. 2) because data points are non-separable by linear classifier in their original input space. On the other hand, after processing the data with the Nonlinear Schrödinger Kernel, a linear classifier can be trained to achieve error-free XOR operation.

Fig. 3 provides results of classification on four datasets: brain ICP (fig. 3a), spoken digits (fig. 3b), and cancer cell images data with two different spectrum readout: time stretch spectrometer (fig. 3c) and grating-based spectrometer (fig. 3d). The datasets are described in the Methods section. The accuracy is calculated using the AUC after a 3-fold cross validation. As a benchmark, we compare the performance of the Nonlinear Schrödinger Kernel with the most commonly used numerical kernel known as the radial basis function kernel (RBF) that is used to perform nonlinear classification with a linear classifier. When applied to the same data, the Nonlinear Schrödinger Kernel reaches an accuracy similar to the numerical RBF kernel. These results and our other results offer the intuition that the processes of spectral modulation and nonlinear evolution perform a conceptually similar task as the kernel commonly used in machine learning applications with a much lower latency as shown in fig. 3e

## Illustration of Exclusive OR (XOR) Inference

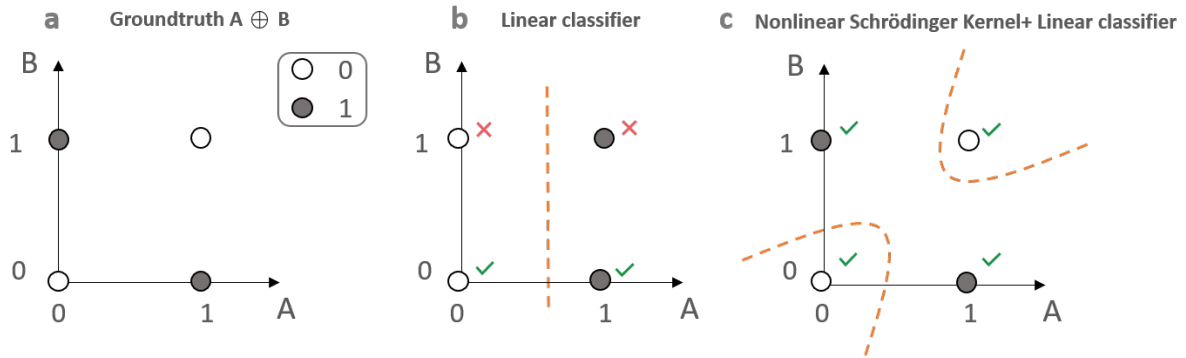


Fig. 2: Experimental demonstration of a nonlinear classification using a linear classifier. The Exclusive OR (XOR) logic is a benchmark nonlinear classification task. The logic states are not linearly separable but our Nonlinear Schrödinger Kernel maps them into a space that is linearly separable. (a) shows the XOR ground truth. (b) shows that a linear classifier (dashed line) cannot correctly produce the output (red crosses denote classification errors). (c) is the linear classifier preceded by the Nonlinear Schrödinger Kernel showing error-free XOR operation.

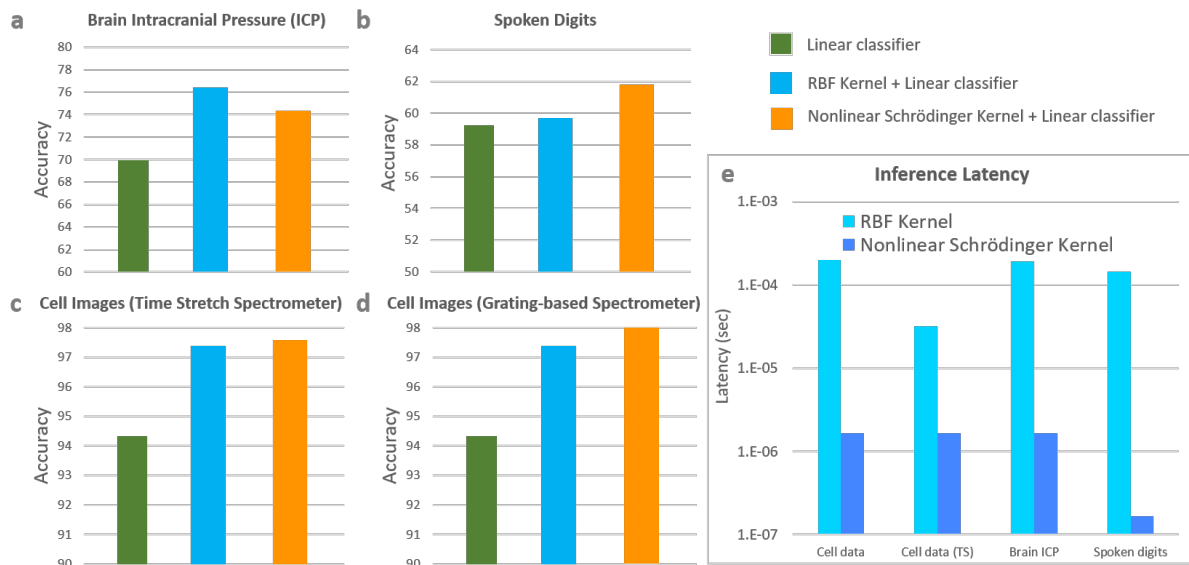


Fig. 3: Illustration of the results of a linear classifier applied on four different datasets: (a) Brain intracranial pressure (ICP) (b) Spoken Digits (c) microscope cancer cell images through a time stretch spectrometer readout (d) microscope cancer cell images through a grating-based spectrometer readout. For each dataset, the AUC is reported after a three-fold cross validation experiment. On the last three datasets (b,c,d), the Nonlinear Schrödinger Kernel outperforms the linear and the RBF kernel classifier. On the first dataset related to brain intracranial pressure (a), the RBF kernel performs the best following by the Nonlinear Schrödinger Kernel and the linear classifier applied to the original data. The Nonlinear Schrödinger Kernel has an improvement that is similar to the one obtained by the RBF kernel when combined with a linear classifier. (e) Bar chart illustration latency for the processing of one sample through an RBF kernel and Nonlinear Schrödinger Kernel. The results are grouped by dataset, including cell data through grating-based spectrometer readout, cell data through time stretch (TS) spectrometer readout, intracranial pressure (ICP), and audio signals recorded from spoken digits. As observed in the bar chart, the latency is in the order of  $1E-4$  to  $1E-5$  seconds for the RBF kernel while the Nonlinear Schrödinger Kernel offers a significantly reduced latency of the order of  $1E-6$  to  $1E-7$

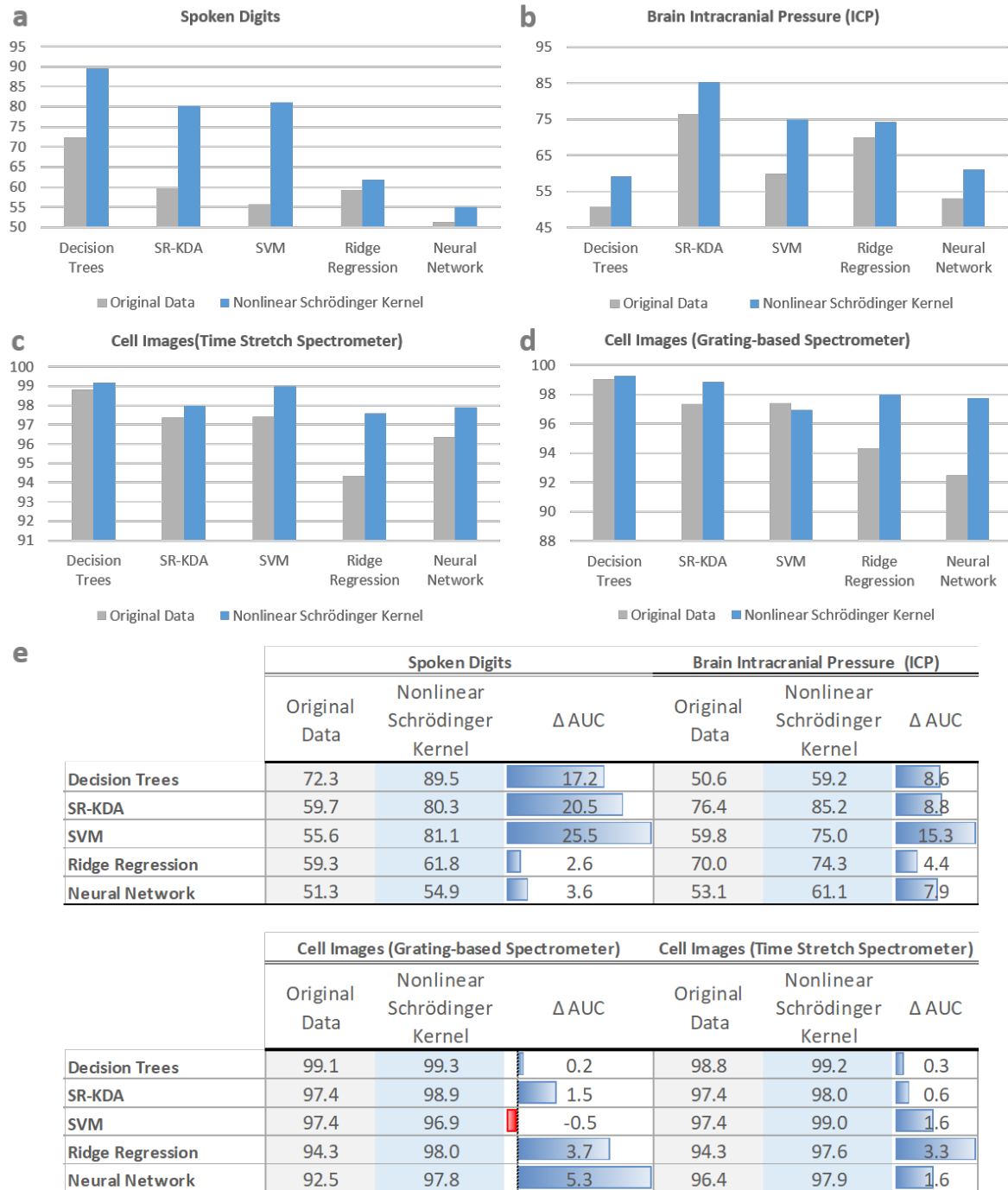


Fig. 4: Classification Results on all datasets each with different machine learning algorithms. The performance of the Nonlinear Schrödinger Kernel in the classification of various datasets (tasks): spoken digit (a), brain ICP (b), cell image data by time stretch spectrometer readout (c), cell image data by a grating-based spectrometer readout (d). For each dataset, we show the performance with and without the Nonlinear Schrödinger Kernel for five different classifiers. The classifiers are: decision tree, spectral regression for kernel discriminant analysis (SR-KDA), support vector machines (SVM), Ridge Regression, and Neural Network. The accuracy in terms of AUC is reported using the raw data as input (gray) and after processing with the Nonlinear Schrödinger Kernel (blue). The improvement by Nonlinear Schrödinger Kernel is consistent for different algorithms and on all datasets. These results show that Nonlinear Schrödinger Kernel can improve the performance of a wide range of machine learning algorithms, both linear and nonlinear. The classification accuracies are quantified in (e).

While fig. 3 highlights the benefit of the Nonlinear Schrödinger Kernel for a linear classifier, we now turn to more advanced machine learning classifiers that already hold nonlinearity in their model including decision trees, spectral regression for kernel discriminant analysis (SR-KDA), support vector machines (SVM), Ridge Regression, and neural network. Specifically, we aim at testing if the Nonlinear Schrödinger Kernel can further improve the result of these already nonlinear classifiers. Fig. 4 summarizes the experimentally measured performance of the Nonlinear Schrödinger Kernel with five different nonlinear classification algorithms. The bar chart illustrates the performance of the kernel with the five classifiers. The AUC is reported using the original data as input (gray) and after processing with the kernel (blue). Consistent improvement in AUC can be observed throughout the different classification methods. An average of 9% improvement in AUC was observed for the brain intracranial pressure. As shown in the table, similar improvement is observed on the additional datasets evaluated (time stretch microscopy cell images and spoken digits datasets) where the Nonlinear Schrödinger Kernel significantly outperforms the original datasets.

## 4. Methods

### 4.1. Datasets

**Continuous Intracranial Pressure (ICP) Waveforms:** Traumatic brain injury (TBI) can lead to secondary brain injury due to pressure effects created by a hematoma and disrupted cerebrospinal fluid circulation. The immediate goal of TBI treatment is minimizing this risk by mitigating elevations in intracranial pressure (ICP). However, due to the wide heterogeneity of the degree of severity of TBI and the difficulty to assess them, the medical management of TBI patients is particularly challenging. This dataset originates from 154 patients [13] admitted for various conditions related to the known risk of intracranial hypertension (IH). The majority of the patients (108 patients) were treated for brain injuries (TBI, subarachnoid hemorrhage (SAH), and intracerebral hemorrhage (ICH)). A total of 63,954 ICP alarms were recorded from bedside monitors. ICP signals were recorded continuously at a sampling rate of 240 Hz using ventriculostomy systems. In our experiments, a random sample of 638 alarms is used. Expert annotation was obtained by a biomedical engineer using dedicated annotation software created in our research laboratory and was asked to label them using the following criterion: an alarm is a false positive if there was no drainage to treat ICP elevation within 15 minutes following the alarm, a true alarm otherwise. This anonymized dataset of ICP signals originates from the University of California, Los Angeles (UCLA) Medical Center, and its usage was approved by the local institutional review board committee (IRB).

**Spoken Digits:** The Free-Spoken Digit Dataset (FSDD) [14] is an audio/speech dataset consisting of 2000 recordings of spoken digits (0-9) in wav files at 8kHz. Each recording contains a spoken digit that was recorded under different conditions and from four different individuals. The recordings were trimmed so that they have near minimal silence at the beginnings and ends. Our classification experiments are posed by considering the classification between digits “zero” and “one”. Each recording is described by 5,000 dimensions.

**Time Stretch Cell Images:** This dataset corresponding to cell images was from time stretch flow through microscope described in [15] [16]. Using a pair of diffraction gratings, a femtosecond laser pulse is converted into a collimated 1-D spatial rainbow. When this spatially and spectrally dispersed pulse illuminates the sample, the spatial information is modulated onto the optical spectrum. Using a low loss dispersive fiber, the spectrum is then mapped into time and stretched such that it is slow enough to be digitized by a realtime analog to digital converter. In order to achieve high sensitivity under single shot operation, the dispersive fiber is pumped to create simultaneous Raman amplification and time stretching. The sample was blood cells flowing serially through a microfluidic channel, and the details of which have been described in our earlier publications [16]. The classification task amounts to differentiating between two cell models: white blood cells (OT-II hybridoma T-cells) and colon cancer cells (SW-480 epithelial) [16]. The dataset corresponds to a random sample of 400 observations equally distributed between the two classes (i.e. normal and cancer). Each data sample is described by 128 dimensions.

### 4.2. Machine Learning Algorithms

**Ridge Regression:** Ridge regression [17] is used in our experiments as a baseline machine learning model. In the context of linear regression, the goal is to fit a function  $f(x_i) = a^T x + b$  to the pairs of training data samples  $(x_i, y_i)$  that minimizes the residual sum of square (RSS):

$$RSS = \sum_{i=1}^n (f(x_i) - y_i)^2$$

By concatenating '1' to each input vector  $x_i$ , the RSS can be written as a vector product:

$$RSS = (X^T a - Y)^T (X^T a - Y)$$

In ridge regression, a regularization term is added based on the norm of the model  $a$ :

$$RSS_{ridge} = \sum_{i=1}^n (a^T x_i - y_i)^2 + \alpha |a|^2 = RSS + \alpha |a|^2$$

where model vector  $a$  is obtained as follows:

$$a = (XX^T + \alpha I)^{-1} Xy$$

and  $I$  is the identity matrix.

**Random Forest:** A random forest [18] is an ensemble learning method that relies on a set of independently trained decision trees. Random forests have successfully been used for classification and regression problems. They operate by constructing multiple decision trees at the training phase, followed by aggregating their results by a majority vote (classification) or averaging (regression). In most applications, the random forest model tends to provide higher accuracy than single decision tree approaches.

In a random forest, each tree is constructed according to a randomly sampled subset of observations and a randomly sampled set of variables. This allows a diverse set of learners that are then averaged, thus reduces the variance associated with a single tree, and decreasing the generalization error. In this work, the trees are constructed by the CART tree fitting method [19]. At each iteration, a set of observations is split into disjoint subsets, such that a loss criterion is minimized. The resulting representation is a tree data structure in which each internal (non-leaf) node is labeled with a variable name and a corresponding split value, while a leaf is labeled with a fitted value; the class label for classification problems, or a numerical value for regression problems.

**Spectral Regression for Kernel Discriminant Analysis (SR-KDA):** Spectral regression (SR-DA) [20] is a method developed to solve discriminant analysis as formulated in ridge regression  $RSS_{ridge}$  but using linear graph embedding (LGE). SR-DA proposes to can first find eigenvector  $y$  by solving  $Wy = \gamma Dy$  and then solve a regularized linear least square problem:

$$\operatorname{argmin}_a \|y - X^T a\|_2 + \gamma \|a\|$$

This two-step process is termed spectral regression (SR) that enjoys two key benefits: 1)  $W$  and  $D$  are usually sparse and hence an efficient algorithm Lanczos is available to obtain eigenvectors; 2) Various matured techniques are available to solve the linear least squares (e.g., ridge regression). SR-DA is an application of SR in solving a supervised learning problem where  $y$  contains class labels for  $X$ . In this case,  $W$  becomes a block-diagonal with  $W_{ij}$  equal to  $1/nc$  when both  $x_i$  and  $x_j$  belong to class  $c$  and  $nc$  is the number samples belonging to class  $c$ . SR-KDA [21] generalizes SR-DA by projecting the input data onto a high-dimensional space via a kernel  $K$ , and class labels  $y$  to obtain vectors  $\alpha$ . This is achieved using a Cholesky decomposition:

$$r = \operatorname{chol}(K + \delta I)$$

$$\alpha = r \setminus (r^T \setminus y)$$

**Support Vector Machines (SVM):** A support vector machine (SVM) [22] is a supervised machine learning technique for classification problems where each sample  $x_i \in X$  is labeled by  $y_i \in \{-1, 1\}$ . SVM aims at finding the optimal separating hyperplane that minimizes the misclassification rate on the training set while maximizing the sum of distances of the training samples from this hyperplane. Formally, this problem accounts for finding the parameter  $\alpha$ , such that:

$$\begin{aligned} & \operatorname{argmin}_\alpha \quad \frac{1}{2} \alpha^T Q \alpha - e^T \alpha \\ & \text{subject to} \quad y^T \alpha = 0 \\ & \quad \quad \quad 0 \leq \alpha_i \leq C, i = 1, \dots, n \end{aligned}$$

where  $C$  is a constant that controls the amount of penalty on the error term during the minimization process,  $e$  is the vector of all ones, and  $Q$  is a matrix defined as:

$$Q_{ij} = y_i y_j K(x_i, x_j)$$

This minimization provides a solution for the following function:

$$f(x) = \sum_{i=1}^n y_i \alpha_i K(x, x_i) + b$$

**Neural Network:** Feedforward networks consist of a series of layers. The first layer has a connection from the network input. Each subsequent layer has a connection from the previous layer. The final layer produces the network's output. Feedforward networks can be used for any kind of input to output mapping. A feedforward network with one hidden layer and enough neurons in the hidden layers can fit any finite input-output mapping problem. By using stochastic gradient descent with momentum (SGDM) optimizer together with cross-entropy loss function, we train a 7-layer feedforward network.

## 5. Summary

Recent breakthroughs in machine learning and advanced computing have given rise to numerous applications of data processing and classification. The need for low-latency data processing frameworks that capture non-linear features of the signal without requiring any training is particularly important in modern technologies related to self-driving vehicles, healthcare, and sensing systems. We have introduced in this paper a data processing framework that utilizes the nonlinear dynamics of an optical system to modulate and process data modulated onto the spectrum. When combined with standard machine learning algorithms, such processing, named Nonlinear Schrödinger Kernel, demonstrates significant improvement in classification accuracy on a wide range of applications at a much lower latency; therefore, offering the best of both worlds. This technique is the spin-off from the photonic time stretch and is fully compatible with time stretch data acquisition [9] for fast single-shot and continuous operation.

## 6. Acknowledgement

This project was supported by the DARPA-MTO PEACH program under contract HR00111990050.

## References

1. Daniel R Solli, Claus Ropers, Prakash Koonath, and Bahram Jalali. Optical rogue waves. *Nature*, 450(7172):1054–1057, 2007.
2. Daniel R Solli, Georg Herink, B Jalali, and Claus Ropers. Fluctuations and correlations in modulation instability. *Nature Photonics*, 6(7):463–468, 2012.
3. Nail Akhmediev, John M Dudley, Daniel R Solli, and SK Turitsyn. Recent progress in investigating optical rogue waves. *Journal of Optics*, 15(6):060201, 2013.
4. Mark C Cross and Pierre C Hohenberg. Pattern formation outside of equilibrium. *Reviews of modern physics*, 65(3):851, 1993.
5. Tingyi Zhou, Fabien Scalzo, and Bahram Jalali. Lambda inference machine: accelerating computing by nonlinear evolution of spectrally modulated data, 2020.
6. Asuri S Bhushan, F Coppinger, and Bahram Jalali. Time-stretched analogue-to-digital conversion. *Electronics Letters*, 34(9):839–841, 1998.
7. Jason Chou, Ozdal Boyraz, Daniel Solli, and Bahram Jalali. Femtosecond real-time single-shot digitizer. *Applied Physics Letters*, 91(16):161105, 2007.
8. K Goda, KK Tsia, and B Jalali. Serial time-encoded amplified imaging for real-time observation of fast dynamic phenomena. *Nature*, 458(7242):1145–1149, 2009.
9. Ata Mahjoubfar, Dmitry V Churkin, Stéphane Barland, Neil Broderick, Sergei K Turitsyn, and Bahram Jalali. Time stretch and its applications. *Nature Photonics*, 11(6):341, 2017.
10. Georg Herink, Felix Kurtz, Bahram Jalali, Daniel R Solli, and Claus Ropers. Real-time spectral interferometry probes the internal dynamics of femtosecond soliton molecules. *Science*, 356(6333):50–54, 2017.
11. Daniel R Solli and Bahram Jalali. Analog optical computing. *Nature Photonics*, 9(11):704–706, 2015.
12. PV Kelkar, F Coppinger, AS Bhushan, and B Jalali. Time-domain optical sensing. *Electronics Letters*, 35(19):1661–1662, 1999.

13. Fabien Scalzo, David Liebeskind, and Xiao Hu. Reducing false intracranial pressure alarms using morphological waveform features. *IEEE Transactions on Biomedical Engineering*, 60(1):235–239, 2012.
14. Zohar Jackson, César Souza, Jason Flaks, Yuxin Pan, Hereman Nicolas, and Adhish Thite. Jakobovski/free-spoken-digit-dataset: v1.0.8, August 2018.
15. Keisuke Goda, Ali Ayazi, Daniel R Gossett, Jagannath Sadasivam, Cejo K Lonappan, Elodie Sollier, Ali M Fard, Soojung Claire Hur, Jost Adam, Coleman Murray, et al. High-throughput single-microparticle imaging flow analyzer. *Proceedings of the National Academy of Sciences*, 109(29):11630–11635, 2012.
16. Claire Lifan Chen, Ata Mahjoubfar, Li-Chia Tai, Ian K Blaby, Allen Huang, Kayvan Reza Niazi, and Bahram Jalali. Deep learning in label-free cell classification. *Scientific reports*, 6:21471, 2016.
17. Arthur E Hoerl and Robert W Kennard. Ridge regression: Biased estimation for nonorthogonal problems. *Technometrics*, 12(1):55–67, 1970.
18. Tin Kam Ho. Random decision forests. In *Proceedings of 3rd international conference on document analysis and recognition*, volume 1, pages 278–282. IEEE, 1995.
19. Leo Breiman, Jerome Friedman, Charles J Stone, and Richard A Olshen. *Classification and regression trees*. CRC press, 1984.
20. Deng Cai, Xiaofei He, and Jiawei Han. Spectral regression for efficient regularized subspace learning. In *2007 IEEE 11th international conference on computer vision*, pages 1–8. IEEE, 2007.
21. Deng Cai, Xiaofei He, and Jiawei Han. Speed up kernel discriminant analysis. *The VLDB Journal*, 20(1):21–33, 2011.
22. Corinna Cortes and Vladimir Vapnik. Support-vector networks. *Machine learning*, 20(3):273–297, 1995.